NANO EXPRESS

Open Access

CrossMark

Anomalous Thermal Expansion of HoCo$_{0.5}$Cr$_{0.5}$O$_3$ Probed by X-ray Synchrotron Powder Diffraction

Vasyl Hreb[1*], Leonid Vasylechko[1], Vitaliya Mykhalichko[1] and Yurii Prots[2]

Abstract

Mixed holmium cobaltite-chromite HoCo$_{0.5}$Cr$_{0.5}$O$_3$ with orthorhombic perovskite structure (structure type GdFeO$_3$, space group *Pbnm*) was obtained by solid state reaction of corresponding oxides in air at 1373 K. Room- and high-temperature structural parameters were derived from high-resolution X-ray synchrotron powder diffraction data collected in situ in the temperature range of 300–1140 K. Analysis of the results obtained revealed anomalous thermal expansion of HoCo$_{0.5}$Cr$_{0.5}$O$_3$, which is reflected in a sigmoidal temperature dependence of the unit cell parameters and in abnormal increase of the thermal expansion coefficients with a broad maxima near 900 K. Pronounced anomalies are also observed for interatomic distances and angles within Co/CrO$_6$ octahedra, tilt angles of octahedra and atomic displacement parameters. The observed anomalies are associated with the changes of spin state of Co^{3+} ions and insulator-metal transition occurring in HoCo$_{0.5}$Cr$_{0.5}$O$_3$.

Keywords: Mixed cobaltites-chromites, Perovskite, Crystal structure, Thermal expansion

Background

Rare earth (*R*) cobaltites *R*CoO$_3$ and chromites *R*CrO$_3$ with perovskite structure due to their high electrical conductivity, specific magnetic properties, as well as significant electrochemical and catalytic activity are considered as prospective electrode and interconnect materials for solid oxide fuel cells (SOFC) [1–3], thermoelectric and magnetocaloric materials [4–6], catalysts and humidity and gas sensors [7–9]. Currently *R*CoO$_3$ and *R*CrO$_3$ compounds and solid solutions on their basis are attracting renewed research interest aroused by their potential application as multifunctional materials [10–13]. *R*CoO$_3$-based materials are of particular interest, due to dependency of their transport, magnetic and other properties on spin state of Co^{3+} ions, which can change with increasing of the temperature from low spin (LS, $t_{2g}^6 e_g^0$, $S = 0$), to intermediate (IS, $t_{2g}^5 e_g^1$, $S = 1$) and high spin (HS, $t_{2g}^4 e_g^2$, $S = 2$) configurations ([14–16] and references herein). These transitions in rare earth cobaltites *R*CoO$_3$ are strongly affected by the chemical pressure caused by cation substitution either in *A*- or *B*-sites of perovskite structure [17–19].

The present work deals with the study of crystal structure of new mixed cobaltite-chromite HoCo$_{0.5}$Cr$_{0.5}$O$_3$ and its thermal behaviour in the temperature range of 300–1140 K by using high-resolution X-ray synchrotron powder diffraction technique. The HoCo$_{0.5}$Cr$_{0.5}$O$_3$ was chosen for the detail structural investigations as a representative of the mixed cobaltites-chromites in view of the fact, that both parent compounds—HoCoO$_3$ and HoCrO$_3$, which are isostructural and isotypic with GdFeO$_3$ [20–23], show a variety of intriguing physical phenomena and properties. In particular, holmium chromite undergoes a low-temperature phase transition from centrosymmetric *Pbnm* to the non-centrosymmetric *Pna*2$_1$ structure, as it was recently suggested by X-ray powder diffraction of HoCrO$_3$ at 80 and 160 K [12]. The authors assume that the polar oxygen rotations of CrO$_6$ octahedra combined with the displacements of Ho in the non-centrosymmetric space group *Pna*2$_1$ engineer ferroelectricity in HoCrO$_3$ below 240 K. For HoCoO$_3$ no structural phase transitions are reported in a broad temperature range between 1.5 and 1098 K, although pronounced anomalies are observed both in low- and

* Correspondence: wasiahreb@meta.ua
[1]Lviv Polytechnic National University, 12 Bandera Street, 79013 Lviv, Ukraine
Full list of author information is available at the end of the article

Springer Open

Hreb *et al. Nanoscale Research Letters* (2017) 12:442

Page 2 of 6

high-temperature lattice expansion [24–26]. A negative expansion observed in *b*-direction (in *Pbnm* setting) below 150 K suggests a magnetoelastic coupling where short-range interactions between Ho^{3+} magnetic moments are established [24]. The high-temperature anomalies are associated with the transitions of the Co^{3+} ions to the higher spin states and coupled metal-insulator transition occurred in $HoCoO_3$ above 780 K [15, 25, 26]. On the assumption of aforesaid extremely complicated structure, magnetic and electronic phase behaviour is expected in the mixed cobaltite-chromite system $HoCo_{0.5}Cr_{0.5}O_3$. Analysis of the thermal expansion behaviour is a very useful tool for the investigation of diverse electronic and magnetic phase transformations occurring in the complex oxide perovskite systems [14, 16, 19].

Methods

$HoCo_{0.5}Cr_{0.5}O_3$ was synthesized by a solid state technique. Precursor oxides Ho_2O_3, Co_3O_4 and Cr_2O_3 were ball-milled in ethanol for 5 h, dried, pressed into pellet and annealed in air at 1373 K for 20 h. After regrinding, the product was repeatedly ball-milled in ethanol for 2 h, dried and annealed in air at 1373 K for 45 h with one intermediate regrinding.

X-ray powder diffraction (Huber imaging plate Guinier camera G670, Cu $K_{\alpha1}$ radiation) was used for the characterization of the sample at room temperature. Thermal behaviour of $HoCo_{0.5}Cr_{0.5}O_3$ crystal structure was studied in situ in the temperature ranges of 300–1140 K by using high-resolution X-ray synchrotron powder diffraction (beamline ID22 at ESRF, Grenoble, France). The data were collected upon the heating of the powdered sample filled into 0.3 mm quartz capillary with the temperature step of 50 K. The wavelength used $\lambda = 0.35434$ Å allows to collect the diffraction data until the maximum $\sin\Theta/\lambda$ value of 0.849 ensuring reliable information on the positional and displacement parameters of atoms in $HoCo_{0.5}Cr_{0.5}O_3$ structure at the elevated temperatures. Corresponding structural parameters were derived by full-profile Rietveld method implemented in the program package WinCSD [27].

Results and Discussion

X-ray powder diffraction examination of new mixed cobaltite-chromite $HoCo_{0.5}Cr_{0.5}O_3$ revealed almost pure perovskite structure isotopic with $GdFeO_3$ (Fig. 1). The obtained values of unit cell dimensions are in excellent agreement with the corresponding data for the parent $HoCoO_3$ and $HoCrO_3$ compounds (Fig. 1, inset 1), thus proving an apparent formation of continuous solid solution $HoCo_{1-x}Cr_xO_3$ with perovskite structure, similarly to the related $RCoO_3$–$RCrO_3$ systems with La, Pr, Nd, Sm, Eu, Gd, Dy, Er and Y [18, 19, 28–33].

In situ high-temperature X-ray synchrotron powder diffraction revealed that $HoCo_{0.5}Cr_{0.5}O_3$ remains
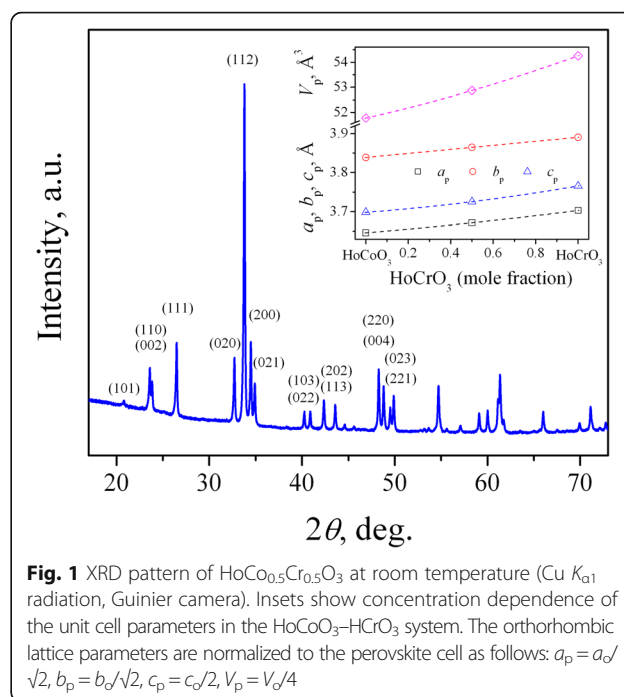
**Fig. 1** XRD pattern of $HoCo_{0.5}Cr_{0.5}O_3$ at room temperature (Cu $K_{\alpha1}$ radiation, Guinier camera). Insets show concentration dependence of the unit cell parameters in the $HoCoO_3$–$HCrO_3$ system. The orthorhombic lattice parameters are normalized to the perovskite cell as follows: $a_p = a_o/\sqrt{2}$, $b_p = b_o/\sqrt{2}$, $c_p = c_o/2$, $V_p = V_o/4$

orthorhombic up to highest investigated temperature of 1140 K. No symmetry-related structural changes were observed. Precise crystal structure parameters of $HoCo_{0.5}Cr_{0.5}O_3$ in the temperature range of 300–1140 K including anisotropic displacement parameters for all atomic positions were derived by full-profile Rietveld refinement. In all cases, the refinement procedure performed in space group *Pbnm* led to the excellent agreement between experimental and calculated profiles. Selected examples of Rietveld refinement at 300 and 1140 K are presented on Fig. 2. Insets on Fig. 2 show corresponding projections of $HoCo_{0.5}Cr_{0.5}O_3$ structure on (001) and (110) planes with thermal ellipsoids of atoms based on the refined structural parameters presented in Table 1.

Crystal structure of $HoCo_{0.5}Cr_{0.5}O_3$ is visualized as 3D framework of corner-shared MO_6 octahedra ($M = Co_{0.5}Cr_{0.5}$) with the Ho atoms occupying hollows between them. The MO_6 octahedra are rather distorted due to displacement of oxygen atoms from their "ideal" positions in the cubic perovskite aristotype. Mutual displacements of oxygen atoms are reflected in the co-operative antiphase tilts of MO_6 octahedra, as is depicted on insets of Fig. 2.

The ratio of the atomic displacement parameters (adps) observed in $HoCo_{0.5}Cr_{0.5}O_3$ structure both at 300 and 1140 K follow well the simple expectation based on the atomic masses, namely $B_{iso/eq}(O) > B_{iso/eq}(Co/Cr) > B_{iso/eq}(Ho)$. Thermal ellipsoids of cations in $HoCo_{0.5}Cr_{0.5}O_3$ structure at room temperature are close to spherical shape, with minor contraction or elongation in *b*-direction:

Hreb *et al. Nanoscale Research Letters* (2017) 12:442

Page 3 of 6
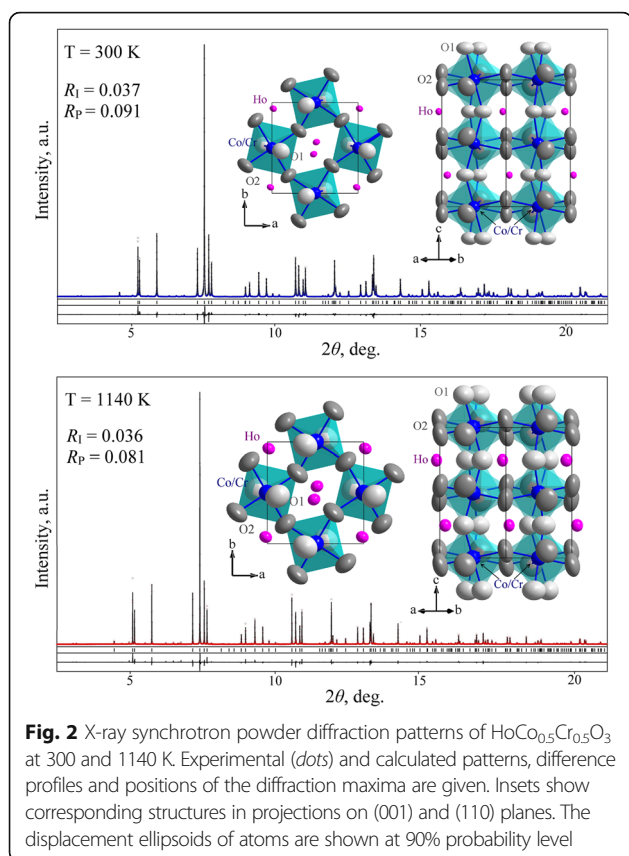
Fig. 2 X-ray synchrotron powder diffraction patterns of $HoCo_{0.5}Cr_{0.5}O_3$ at 300 and 1140 K. Experimental (*dots*) and calculated patterns, difference profiles and positions of the diffraction maxima are given. Insets show corresponding structures in projections on (001) and (110) planes. The displacement ellipsoids of atoms are shown at 90% probability level

behaviour along M–O bonds (Fig. 2, insets). At the elevated temperatures, the displacement ellipsoids for Co/Cr atoms become almost spherical, whereas those for Ho^{3+} species exhibit considerable anisotropy, e.g. $B_{33} > B_{11} > B_{22}$ at 1140 K. The behaviour of adps of oxygen species located in $4c$ and $8d$ sites ($B_{11} \approx B_{22} > B_{33}$ and $B_{11} \approx B_{22} < B_{33}$, respectively) does not change with the temperature (Table 1). However, it can be noticed that displacement parameters of apical O1 atoms located in $4c$ sites become more isotropic at the elevated temperatures (Fig. 2, insets).

Analysis of the thermal behaviour of $HoCo_{0.5}Cr_{0.5}O_3$ structure revealed pronounced anomalies in the lattice expansion, which are reflected in a sigmoidal temperature dependence of the unit cell dimensions and in significant increase of the thermal expansion coefficients (TECs) with broad maxima around 900 K (Fig. 3). Similar abnormal lattice parameter behaviour was earlier observed in the related mixed cobaltites-chromites $LaCo_{1-x}Cr_xO_3$ [28] and $RCo_{0.5}Cr_{0.5}O_3$ (R = Pr, Sm, Eu, Gd, Dy and Er) [19, 31–33].
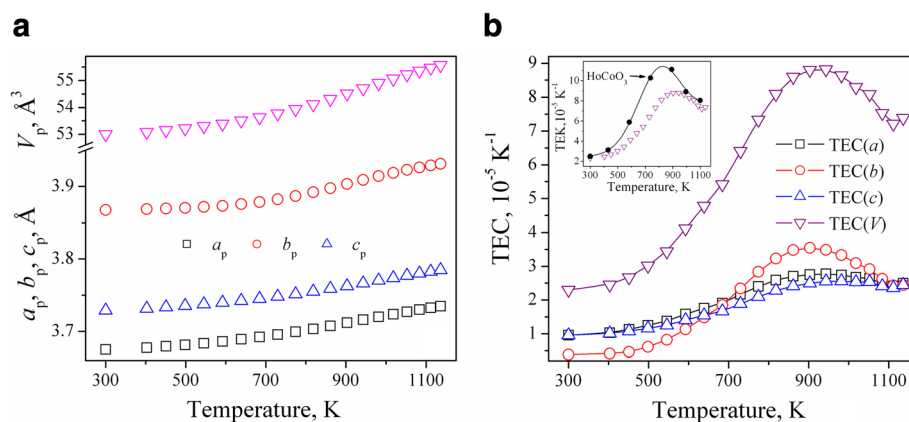
In the "pure" rare earth cobaltites $RCoO_3$ abnormal thermal behaviour of the lattice expansion is associated with magnetic phase transitions and with a change of electronic configuration and spin state of Co^{3+} ions, which lead to the increment of the lattice parameters and unit cell volume due to increase of the radii of Co^{3+} ions in the exited states (r(LS) = 0.545 Å, r(IS) = 0.560 Å, r(HS) = 0.610 Å). The maxima at the temperature dependence of the thermal expansion coefficients in rare earth cobaltites show clear correlation with the temperature of insulator–metal transition, obtained from resistivity measurements, which increases in the $RCoO_3$ series from 535 K for $LaCoO_3$ to 785 and 800 K for $DyCoO_3$ and $YCoO_3$, respectively [14].

It is assumed that the observed structural anomalies in $HoCo_{0.5}Cr_{0.5}O_3$ around 900 K are also associated with

$B_{11} \approx B_{33} > B_{22}$ for Ho^{3+} and $B_{11} \approx B_{33} < B_{22}$ for Co^{3+}/Cr^{3+}. More pronounced anisotropic behaviour is observed for the displacement parameters of oxygen species, reflected in the remarkable contraction or elongation of the corresponding ellipsoids in c-direction (Table 1). Thermal ellipsoids of oxygen atoms both in equatorial ($8d$) and apical ($4c$) positions of MO_6 octahedra show near rotation-type

Table 1 Coordinates and atomic displacement parameters in $HoCo_{0.5}Cr_{0.5}O_3$ structure (space group *Pbnm*) at 300 and 1140 K

Parameters	Ho, 4c		Co/Cr, 4b		O1, 4c		O2, 8d	
	300 K	1140 K	300 K	1140 K	300 K	1140 K	300 K	1140 K
x/a	−0.01617(9)	−0.0155(2)	0		0.1043(9)	0.1074(11)	−0.3090(7)	−0.3130(9)
y/b	0.06694(8)	0.0654(1)	½		0.4670(9)	0.4675(12)	0.3057(7)	0.3061(9)
z/c	¼		0		¼		0.0541(5)	0.0539(6)
B_{eq}^a	0.556(8)	1.52(2)	1.65(3)	2.63(5)	2.9(2)	5.0(3)	3.14(14)	4.7(2)
B_{11}	0.61(2)	1.53(3)	1.64(5)	2.68(8)	3.6(3)	5.7(5)	2.9(2)	4.2(3)
B_{22}	0.48(2)	1.33(2)	1.74(5)	2.64(9)	3.2(3)	5.2(5)	2.5(2)	3.8(3)
B_{33}	0.58(2)	1.72(3)	1.56(5)	2.57(7)	1.9(3)	4.2(4)	4.0(3)	6.1(4)
B_{12}	−0.07(2)	−0.13(4)	0.05(6)	−0.03(10)	0.2(3)	0.6(4)	−1.0(2)	−1.4(3)
B_{13}	0		−0.04(6)	−0.04(10)	0		0.5(2)	−0.2(3)
B_{23}	0		−0.02(4)	0.03(5)	0		−0.3(2)	−0.8(3)
Lattice parameters	a = 5.19695(8) Å, b = 5.46911(8) Å, c = 7.45765(9) Å (at 300 K)							
	a = 5.28195(7) Å, b = 5.55944(7) Å, c = 7.56949(9) Å (at 1140 K)							

$^aB_{iso/eq}$ = 1/3[$B_{11}(a^*)^2a^2$ + … $2B_{23}b^*c^*bc$ cosα]; displacement factors are defined as exp[−1/4(B_{11} $(a^*)^2$ h^2 + … $2B_{23}b^*c^*k$ l)]

Hreb *et al. Nanoscale Research Letters* (2017) 12:442

Page 4 of 6

Fig. 3 Temperature evolution of the normalized unit cell parameters (**a**) and linear thermal expansion coefficients (**b**) of HoCo$_{0.5}$Cr$_{0.5}$O$_3$. The orthorhombic lattice parameters are normalized to the perovskite cell as follows: $a_p = a_o/\sqrt{2}$, $b_p = b_o/\sqrt{2}$, $c_p = c_o/2$, $V_p = V_o/4$. The values on linear TECs in three crystallographic directions as well volumetric TEC were obtained by differentiation of experimental unit cell dimensions on the temperature. Inset on the *right panel* shows volumetric TEC of HoCo$_{0.5}$Cr$_{0.5}$O$_3$ in comparison with literature data for HoCoO$_3$ [25]

the magnetic and electronic phase transitions occurred at the elevated temperatures in the end members of this system. In particular, according to the electronic phase diagram of the RCoO$_3$ perovskites [15], HoCoO$_3$ undergoes a transition from nonmagnetic dielectric to paramagnetic dielectric state at 486 K and insulator–metal transition at 782 K. Detected anomalies in the lattice expansion of the mixed cobaltite-chromite HoCo$_{0.5}$Cr$_{0.5}$O$_3$ are less pronounced than in the "pure" HoCoO$_3$ [25], whereas the maximum at TEC curve is shifted to the higher temperatures (inset of Fig. 3b). Similar effect of cationic exchange was observed in the related RCoO$_3$–RCrO$_3$ systems, where increasing chromium content in NdCo$_{1-x}$Cr$_x$O$_3$ and GdCo$_{1-x}$Cr$_x$O$_3$ series led to increase of the temperature of metal–isolator transitions [18, 30].

Thorough analysis of the selected bond length, atomic displacement parameters and octahedral tilt angles in HoCo$_{0.5}$Cr$_{0.5}$O$_3$ structure indicates additional structural anomalies, which are evidently associated with the electronic and magnetic phase transitions occurring in the HoCoO$_3$–HoCrO$_3$ system at elevated temperatures. Temperature evolution of the M–O bond lengths in the HoCo$_{0.5}$Cr$_{0.5}$O$_3$ structure is presented on Fig. 4a. Initially, both M–O1 and M–O2 distances remain practically unchanged. Significant change in configuration of MO$_6$ octahedra occurs between ~600 and 850 K, where an excitation to the higher spin states of Co^{3+} ions begins. Detectable deviation from the "normal" behaviour in this temperature range is also observed for the temperature dependence of the displacement parameters of oxygen species in HoCo$_{0.5}$Cr$_{0.5}$O$_3$ structure (Fig. 4b). Further increasing of the temperature led to the increase of all M–O distances and to the convergence of both sets of M–O2 bond lengths in the equatorial plane of MO$_6$ octahedra (Fig. 4a). Thus, the shape of MO$_6$

octahedra at the elevated temperatures differs considerably from the room temperature configuration.

Temperature evolution of the M–O1–M and M–O2–M bond angles in HoCo$_{0.5}$Cr$_{0.5}$O$_3$ structure reflecting the magnitude of MO$_6$ octahedral tilt angles along [110] and [001] axis (Fig. 5a) displays clear divergence behaviour. The M–O2–M angles systematically decrease with increasing the temperature, whereas M–O1–M angles show increasing behaviour with detectable discontinuity between 770 and 900 K.

It is known that the M–O–M bong angles (θ) in RMO$_3$ perovskite series characterize the M^{3+}–O^{2-}–M^{3+} overlaps and govern the magnetic and transport properties of rare earth manganites, nickelates and cobaltites [34, 35]. In particular, increase of cooperative rotations of corner-shared CoO$_6$ octahedra in RCoO$_3$ perovskites led to reducing of Co–O–Co bond angles and the bandwidth of Co(3d)–O(2p) interactions, which are correlated with the increasing spin-state transition temperature, T_{onset} [15]. According to ([15, 35] and references herein), in the RCoO$_3$ cobaltite series the σ^*-bonding e_g bandwidth $W \propto \cos\omega/\langle\text{Co–O}\rangle^{3.5}$, where $\omega = (180 - \langle\theta\rangle)/2$ is the average octahedral tilting angle, and $\langle$Co–O$\rangle$—the mean bond length inside CoO$_6$ octahedra. The broadening of W in rare earth cobaltite series reduces the spin gap and decreases the onset of spin transition of Co^{3+} from LS to IS state [15]. Figure 5b demonstrates the temperature dependence of the inverse bandwidth, W^{-1} of HoCo$_{0.5}$Cr$_{0.5}$O$_3$, which increase with the temperature solely due to increase of the average bond lengths inside octahedra, whereas the octahedral tilt angles are practically temperature independent (Fig. 5b, inset). Observed increasing behaviour of the inverse bandwidth of HoCo$_{0.5}$Cr$_{0.5}$O$_3$ clearly illustrates an increasing population of the exited spin states of Co^{3+} ions with the

Hreb et al. Nanoscale Research Letters (2017) 12:442

Page 5 of 6
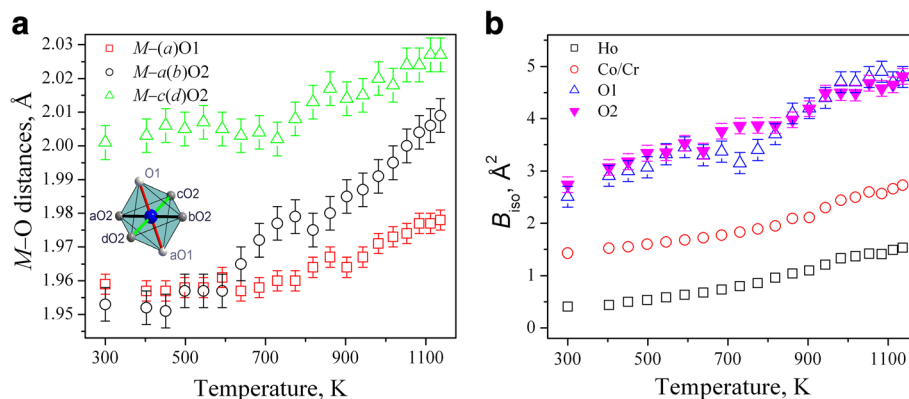
Fig. 4 Temperature evolution of M–O bond lends (**a**) and isotropic displacement parameters of atoms (**b**) in $HoCo_{0.5}Cr_{0.5}O_3$ structure

temperature. It is apparent that the magnetic and electrical properties of $HoCo_{0.5}Cr_{0.5}O_3$ will depend on the spin state of the Co^{3+} ions and a cation–anion–cation overlap, as it was reported for the related $NdCo_{1-x}Cr_xO_3$ and $GdCo_{1-x}Cr_xO_3$ systems [18, 30]. Increasing structural deformation in the last systems caused by the substitution of chromium by cobalt shifts the onset of Co^{3+} spin excitations and metal-insulator transition to the highest temperatures and led to the rising of electrical conductivity and Néel temperature in $NdCo_{1-x}Cr_xO_3$ series. It is evident that the coupling of the electronic and magnetic transitions combined with the anomaly of the lattice behaviour will result in extremely complicated magnetic and electronic phase diagram of the mixed cobaltite-chromite systems.

Conclusions

Crystal structure parameters of the mixed holmium cobaltite-chromite $HoCo_{0.5}Cr_{0.5}O_3$ synthesized by solid state reaction in air at 1373 K have been studied in the temperature range of 300–1140 K by using high-resolution X-ray synchrotron powder diffraction technique. Experimental X-ray synchrotron powder diffraction patterns and crystal structure parameters of $HoCo_{0.5}Cr_{0.5}O_3$ structure at room temperature and 1140 K are published by the International Centre of Diffraction Data (ICDD) in the last release of the Powder Diffraction File (PDF cards NN 00-066-0678 and 00-066-0679, respectively). Detailed analysis of the temperature dependence of structural parameters revealed pronounced anomalies in thermal behaviour of the unit cell dimensions and thermal expansion coefficients with clear maxima at around 900 K. Extra structural anomalies are also observed on temperature dependencies of the M–O bond lengths, octahedral tilt angles and atomic displacement parameters, which are evidently caused with the temperature induced changes of spin configuration of Co^{3+} ions and coupled metal-insulator transition occurred in $HoCoO_3$–$HoCrO_3$ system.
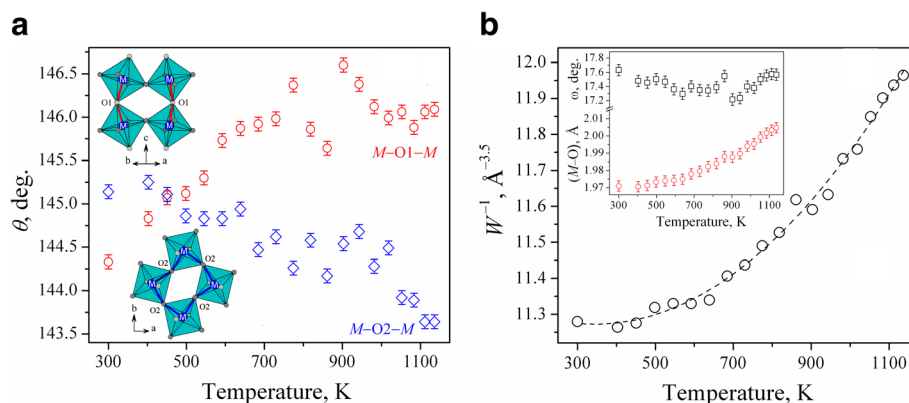
Fig. 5 Temperature evolution of the M–O–M angles (**a**) and inverse bandwidth W^{-1} (**b**) in $HoCo_{0.5}Cr_{0.5}O_3$ structure. Inset shows thermal behaviour of the average bong length M–O and octahedral tilt angles

Hreb *et al. Nanoscale Research Letters* (2017) 12:442

Page 6 of 6

Publisher's Note
Springer Nature remains neutral with regard to jurisdictional claims in published maps and institutional affiliations.

Author details
[1]Lviv Polytechnic National University, 12 Bandera Street, 79013 Lviv, Ukraine. [2]Max-Planck-Institut für Chemische Physik fester Stoffe, Nöthnitzer Str. 40, 01187 Dresden, Germany.

References
1. Uhlenbruck S, Tietz F (2004) High-temperature thermal expansion and conductivity of cobaltites: potentials for adaptation of the thermal expansion to the demands for solid oxide fuel cells. Mater Sci Eng B 107:277–282
2. Tsipis EV, Kharton VV (2008) Electrode materials and reaction mechanisms in solid oxide fuel cells: a brief review II. Electrochemical behavior vs. materials science aspects. J Solid State Electrochem 12:1367–1391
3. Fergus JW (2004) Lanthanum chromite-based materials for solid oxide fuel cell interconnects. Solid State Ion 17:1–15
4. Moon JW, Masuda Y, Seo WS, Koumoto K (2001) Influence of ionic size of rare-earth site on the thermoelectric properties of $RCoO_3$-type perovskite cobalt oxides. Mater Sci Eng B 85:70–75
5. Inagoya A, Sawaki D, Horiuchi Y, Urata S, Funahashi R, Terasaki I (2011) Thermoelectric module made of perovskite cobalt oxides with large thermopower. J Appl Phys 110:123712
6. Gupta P, Poddar P (2016) Study of magnetic and thermal properties of $SmCrO_3$ polycrystallites. RSC Adv 6:82014–82023
7. Gilbu Tilset B, Fjellvag H, Kjekshus A, Slagtern A, Dahl I (1996) Properties of $LaCo_{1-t}Cr_tO_3$. III. Catalytic activity for CO oxidation. Appl Catal A 147:189–205
8. Alifanti M, Bueno G, Parvulescu V, Parvulescu VI, Cortes CV (2009) Oxidation of ethane on high specific surface $SmCoO_3$ and $PrCoO_3$ perovskites. Catal Today 143:309–314
9. Michel CR, Delgado E, Santillán G, Martínez AH, Chávez-Chávez A (2007) An alternative gas sensor material: synthesis and electrical characterization of $SmCoO_3$. Mater Res Bull 42:84–93
10. Sahu JR, Serrao CR, Ray N, Waghmare UV, Rao CNR (2007) Rare earth chromites: a new family of multiferroics. J Mater Chem 17:42–44
11. Preethi Meher KRS, Martin C, Caignaert V, Damay F, Maignan A (2014) Multiferroics and magnetoelectrics: a comparison between some chromites and cobaltites. Chem Mater 26(Suppl 1):830–836
12. Ghosh A, Pal A, Dey K, Majumdar S, Giri S (2015) Atypical multiferroicity of $HoCrO_3$ in bulk and film geometry. J Mater Chem C 3:4162
13. Talley KR, Barron SC, Nguyen N, Wong-Ng W, Martin J, Zhang YL, Song X (2017) Thermoelectric properties of the $LaCoO_3 – LaCrO_3$ system using a high-throughput combinatorial approach. Solid State Sci 64:7–12
14. Knížek K, Jirák Z, Hejtmánek J, Veverka M, Maryško M, Maris G, Palstra TTM (2005) Structural anomalies associated with the electronic and spin transitions in $LnCoO_3$. Eur Phys J B 47:213–220
15. Tachibana M, Yoshida T, Kawaji H, Atake T, Takayama-Muromachi E (2008) Evolution of electronic states in $RCoO_3$ (R = rare earth): Heat capacity measurements. Phys Rev B 77:094402
16. Berggold K, Kriener M, Becker P, Benomar M, Reuther M, Zobel C, Lorenz T (2008) Anomalous expansion and phonon damping due to the Co spin-state transition in $RCoO_3$ (R = La, Pr, Nd, and Eu). Phys Rev B 78:1–15
17. Baier J, Jodlauk S, Kriener M, Reichl A, Zobel C, Kierspel H, Freimuth A, Lorenz T (2005) Spin-state transition and metal-insulator transition in $La_{1-x}Eu_xCoO_3$. Phys Rev B 71:014443–10
18. Taguchi H (1996) Spin state of cobalt ion in $Nd(Cr_{1-x}Co_x)O_3$. J Solid State Chem 122:297–302
19. Vasylechko L, Bell AMT. Influence of cation substitution on spin-state transitions in mixed RE cobaltites and chromites. Proceedings of the International Conference on Oxide Materials for Electronic Engineering – fabrication, properties and applications (OMEE-2012). September 3–7, 2012, Lviv, Ukraine. Lviv, Publishing House of Lviv Polytechnic, 2012, p. 103–104. IEEE Conference publications; doi:10.1109/OMEE.2012.6464781
20. Demazeau G, Pouchard M, Hagenmuller P (1974) Sur de nouveaux composes oxygenes du cobalt + III derives de la perovskite. J Solid State Chem 9:512
21. Alonso JA, Martınez-Lope MJ, de la Calle C, Pomjakushin V (2006) Preparation and structural study from neutron diffraction data of $RCoO_3$ (R = Pr, Tb, Dy, Ho, Er, Tm, Yb, Lu) perovskites. J Mater Chem 16:1555–1560
22. Kuznetsov MV, Parkin IP (1998) Convenient rapid synthesis of rare earth orthochromites $LnCrO_3$ by self-propagating high-temperature synthesis. Polyhedron 6:3332–3349
23. Tiwari B, Surendra MK, Rao MSR (2013) $HoCrO_3$ and $YCrO_3$: a comparative study. J Phys Condens Matter 25:216004
24. Muñoz A, Martínez-Lope MJ, Alonso JA, Fernández-Díaz MT (2012) Magnetic structures of $HoCoO_3$ and $TbCoO_3$. Eur J Inorg Chem 35:5825–5830
25. Liu X, Prewitt CT (1991) High-temperature diffraction study of $LnCoO_3$ perovskites: a high-order electronic phase transition. J Phys Chem Solids 52:44–448
26. Zhu Z, Gua J, Jia Y, Hu X (2010) Influence of Co–O bond length on the spin state of Co in cobaltite perovskites $RCoO_3$ (R = Y, Ho). Phys Status Solidi B 247:308–312
27. Akselrud L, Grin Y (2014) WinCSD: software package for crystallographic calculations (version 4). J Appl Crystallogr 47:803–805
28. Gilbu Tilset B, Fjellvag H, Kjekshus A (1994) Properties of $LaCo_{1-t}Cr_tO_3$. I. Solid solubility, thermal expansion and structural transition. Acta Chem Scand 48:37–45
29. Dimitrovska-Lazova S, Kovacheva D, Aleksovska S, Marinšek M, Tzvetkov P (2012) Synthesis and structural details of perovskites within the series $PrCo_{1-x}Cr_xO_3$ (x = 0, 0.33, 0.5, 0.67 and 1). Bulgarian Chemical Communications 44:37–46
30. Pecovska-Gjorgjevich M, Aleksovska S, Marinšek M, Dimitrovska-Lazova S (2014) Impedance and AC Conductivity of $GdCr_{1-x}Co_xO_3$ (x = 0, 0.33, 0.5, 0.67 and 1) Perovskites. J Am Ceram Soc 97:3864–3871
31. Vasylechko L, Kuz O, Kharko O, Prots Y, Senyshyn A, Bell A (2011) Anomalous lattice expansion of new mixed cobaltites-chromites $RCo_{0.5}Cr_{0.5}O_3$ (R = Pr, Sm, Eu, Gd). Photon Science - HASYLAB Annual Report., http://photon-science.desy.de/annual_report/files/2011/20111602.pdf
32. Vasylechko L, Pekinchak O, Hreb V, Yu P, Chernyshov D, Fitch A (2017) Anomalous thermal behaviour of mixed cobaltites-ferrites and cobaltites-chromites. Solid State Phenomena 257:99–102
33. Hreb V, Vasylechko L. New mixed perovskites $RCo_{0.5}Cr_{0.5}O_3$ (R = Dy, Ho, Er) as potential thermoelectric and sensory materials. 6th International Youth Science Forum LITTERIS ET ARTIBUS 2016. November 24–26, 2016, Lviv, Ukraine. Proceedings, p. 47–48
34. Goodenough JB, Zhou JS, Rivadulla F, Winkler E (2003) Bond-length fluctuations in transition-metal oxoperovskites. J Solid State Chem 175:116–123
35. Zhou JS, Yan JQ, Goodenough JB (2005) Bulk modulus anomaly in $RCoO_3$ (R = La, Pr, and Nd). Phys Rev B 71:220103